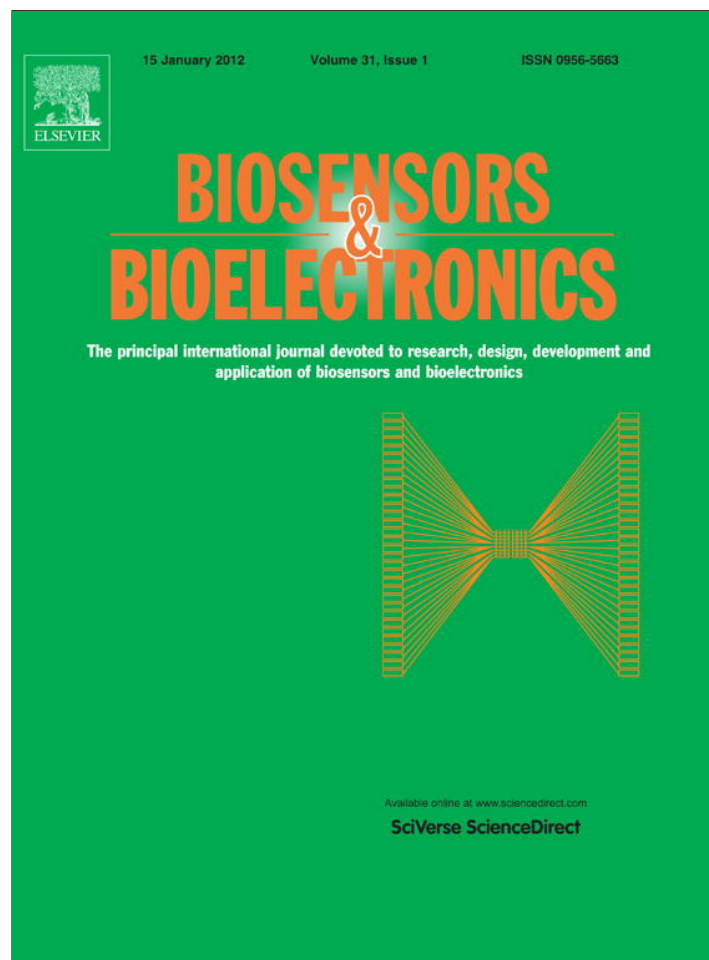


Provided for non-commercial research and education use.
Not for reproduction, distribution or commercial use.



This article appeared in a journal published by Elsevier. The attached copy is furnished to the author for internal non-commercial research and education use, including for instruction at the authors institution and sharing with colleagues.

Other uses, including reproduction and distribution, or selling or licensing copies, or posting to personal, institutional or third party websites are prohibited.

In most cases authors are permitted to post their version of the article (e.g. in Word or Tex form) to their personal website or institutional repository. Authors requiring further information regarding Elsevier's archiving and manuscript policies are encouraged to visit:

<http://www.elsevier.com/copyright>

Contents lists available at [SciVerse ScienceDirect](http://www.sciencedirect.com)

Biosensors and Bioelectronics

journal homepage: www.elsevier.com/locate/bios

Chopper-stabilized gas chromatography-electroantennography: Part I. Background, signal processing and example

Andrew J. Myrick*, Thomas C. Baker

Dept. of Entomology, Center for Chemical Ecology, 104 Chemical Ecology Laboratory, Penn State University, University Park, PA 16802, USA

ARTICLE INFO

Article history:

Received 15 July 2011

Received in revised form 10 October 2011

Accepted 11 October 2011

Available online 19 October 2011

Keywords:

GC-EAD

Electroantennogram

Chopper stabilization

Lock-in amplifier

Pheromone

Chemical ecology

ABSTRACT

A new method that can improve gas-chromatography-electroantennographic detection (GC-EAD) by orders of magnitude through a technique known as chopper stabilization combined with matched filtering in colored noise is presented. The EAD is a physiological recording from the antenna of an insect which can be used to find compounds in the GC effluent that the antenna is able to detect, having important applications for pest control and understanding of chemical communication in nature. The new method is demonstrated with whole-animal male *Helicoverpa zea* antennal preparations for detection of major pheromone component (cis-11-hexadecenal) and compared to results obtained using traditional EAD recording techniques. Results indicate that chopper stabilization under these circumstances can increase odorant detection performance by a factor of approximately 10^4 over traditional methods. The time course of the response of the antenna is also better resolved under chopped conditions. Although the degree of improvement is expected to vary with insect species, odor, and insect preparation, under most circumstances a more sensitive and robust GC-EAD instrument will result from the application of this technique.

© 2011 Elsevier B.V. All rights reserved.

1. Introduction

Combination of the electroantennogram (EAG) (Schneider, 1957) with gas chromatography (GC) (Moorhouse et al., 1969) (and subsequently mass-spectroscopy) allows identification of the specific volatile compounds that give rise to a physiological response in insects. The electroantennogram (EAG) is the electrical potential measured between the ends of the antenna of an insect. Combination of the two techniques is accomplished by splitting the GC effluent and passing it simultaneously over both an insect antenna and conventional GC detector such as a flame ionization detector (FID). GC peaks that elicit a response in the insect may then be identified. Early application of the GC-EAD permitted the identification of a large number of pheromonal components (Struble and Arn, 1984) and is still being used with success for this purpose (Sillam-Dussès et al., 2009). Recently, GC-EAD has become an important tool to study inter-species interactions in the field of chemical ecology (Schiestl and Marion-Poll, 2002). Studies that employ GC-EAD measurements in the field of chemical ecology are numerous. For instance, fruit fly GC-EADs were performed on host fruit volatile collections to determine which components gave significant physiological responses (Siderhurst and Jang, 2006). In Olsson et al. (2005), GC-EAD recordings were made from the moths

Ephestia cautella and *Plodia interpunctella* to volatiles in chocolate. In Zhang et al. (2008), GC-EAD measurements were made in pursuit of active compounds involved in chemical communications between beetles, their predators and host plant volatiles.

Non-pheromonal compounds (such as plant volatiles) tend to result in smaller EAG signals that can be masked by noise and hence techniques that increase the signal to noise ratio (SNR) are desirable. In the past, several antennae connected in series or in parallel were used to increase SNR (Park and Baker, 2002). Also, steps towards the automated recognition of EAD depolarizations were taken in (Sloane and Sullivan, 2007). Here, matched filtering in colored noise (Helstrom, 1960; Moon and Stirling, 2000; Srinath and Rajasekaran, 1979; Trees, 2001) was applied, which increases SNR using knowledge of the shape of an EAD depolarization and the covariance of the noise, simultaneously providing a convenient way to estimate signal amplitude.

Modulation has been used to some extent in EAD recordings. In fact, out of necessity, (Moorhouse et al., 1969) modulated at 0.07 Hz with a 20% duty cycle in the original GC-EAD experiments. Later, Gouinguéné et al. (1998) thermally modulated the capillary column at 0.33 Hz with a 27% duty cycle. In those studies, more favorable modulation frequencies were not possible. Here, we demonstrate the use of modulation at a frequency of 8 Hz combined with demodulation to dramatically increase the SNR obtained from GC-EAD recordings. Such a technique has been widely used in other applications and is sometimes known as chopper stabilization or lock-in amplification. We performed an experiment involving detection of

* Corresponding author. Tel.: +1 814 863 3877.

E-mail address: ajm25@psu.edu (A.J. Myrick).

major pheromone component, Z11-16:Ald, using male antennae of live, whole animal, *H. zea* preparations. Results are tabulated and displayed visually. Relevant background information about the EAG, chopper stabilization, and GC-EAD is also summarized.

1.1. The electroantennogram (EAG)

There are a variety of reported methods for making EAG measurements, including different techniques for making electrical contact to the antenna as well as ways to prepare the insect. The insect may remain intact, or the antenna or entire head may be excised (Malo et al., 2000; Schiestl and Marion-Poll, 2002). Typically, electrical contact with the antenna is made with saline (Kaissling, 1995; Malo et al., 2000; Roelofs, 1984; Struble and Arn, 1984) but electro-conductive gel may also be used (Guédot et al., 2008). An antenna may even be connected directly, via saline, to the gate of a field-effect transistor (Schroth et al., 1999; Ziegler et al., 1998). These investigators (Schroth et al., 2001b) were also able to use different insect species' antennae in an electronic nose configuration.

In general, when a relevant odor is passed over an antenna, a negative deflection is observed on the EAG up to several millivolts on top of a drifting offset in the hundreds of millivolts where the observed deflection is a function of the concentration and time course of the odorant environment. According to Kaissling (1995), the EAG is due to the summation of many dipoles oriented in the axial direction created by sensory neurons. Modeling the transduction properties of the antenna is difficult because they are non-linear and time varying due to accommodation and other factors. For instance, long-term adaptation of the EAG to exposure to major pheromone component is demonstrated in Stelinski et al. (2003). Single sensillum recordings illustrate adaptation in the *Manduca sexta* (Dolzer et al., 2003). Even interactions with other odors affect the response to pheromones (Party et al., 2009). Characteristics of the antennal response are also stimulus-compound dependent (Schuckel et al., 2008). We also found the frequency response was concentration dependent (Myrick and Baker, in preparation).

At frequencies above 1 Hz in *Drosophila*, the EAG voltage is well approximated by a linear single pole low-pass filter at an operating point (Schuckel and French, 2008; Schuckel et al., 2008). Transiently, rise times can be as low as 4.4 ms (Schuckel et al., 2008), with a -3 dB upper corner frequency (at an operating point of constant average concentration) of approximately 13 Hz.

Measurements of the passive properties of excised potato beetles' antennae have been made through spectroscopic impedance measurements (Schroth et al., 2001a). This investigation supported a parallel resistor-capacitor electrical model for the antenna, but at frequencies of interest (<100 Hz) was resistive in the range of several mega-ohms.

Studies that attempt to correlate the response of the antenna to a specific amount of odorant generally refer to "dose response" relationships (Olsson et al., 2005). For instance in Patte et al. (1989), several empirical dose-response models with a limited number of parameters are fit to experimental data obtained from honey bees. Also see Mankin and Mayer (1983) for an empirical model relating dose and action potential rates in single sensillum recordings.

Other less empirical models that account for the physical processes occurring during transduction have also been proposed. A physiologically based electrical model for the American cockroach background potential and EAG was postulated in Kapitskii and Gribakin (1992). In Rospars et al. (2000), the transport of the odorant to the receptor, its binding and deactivation were accounted for.

Noise arises from inside the antenna, which not only contains chemo-receptors, but mechanical receptors and hygroreceptors as

well (Kaissling, 1995). As air is swept across the antenna, mechano-receptors are stimulated. The amount of noise is also affected by humidity, being quieted by high humidity. Background neural activity as part of the normal functioning of the antenna and responses to unknown odors also produce noise. In live insect preparations, additional electrical noise arises from neurons and muscle cells that are not in the antenna.

The amount of noise measured across the antenna is strongly affected by the type of preparation used. Measured noise power spectral densities (PSDs) for three preparation types from DC to 35 Hz are shown in Fig. 1(A). These recordings were made using the system described in Section 3. The three preparation types depicted include two types where the antenna is excised from the insect and one where the whole insect is used. The excised types differ in the way the electrical connection is made to the antenna, either through electroconductive gel or saline. The differing amounts of noise between types of preparations is a subject of speculation. For instance, gel tends to coat the hydrophobic cuticle, which is capacitively coupled to many "noisy" sensilla that could be reacting to the gel itself. In live preparations, noise due to neurons and muscle cells outside of the antenna are an additional source of noise.

In our recordings, the noise below approximately 1–2 Hz down to less than 0.1 Hz, perhaps lower, tends to be "Brownian" in the frequency domain. Although EAD noise is not Brownian due to its non-Gaussian and non-stationary characteristics, Brownian noise results when white Gaussian noise is integrated in time, resulting in a PSD that is proportional to $1/f^2$. Recordings made outdoors on live insects have PSDs that are proportional to $1/f^2$ all the way down to approximately 1 mHz (unpublished data). This should be interpreted with caution because the EAG signal is also a function of atmospheric turbulence and background odors present outdoors.

The quantile–quantile (Q–Q) plots in Fig. 1(B) illustrate non-Gaussian behavior of EAD noise in matched filtered recordings obtained from excised *Helicoverpa subflexa* saline-connected antennae (see Myrick and Baker, in preparation) for experimental details). It can be seen that the chopped and demodulated data (8 Hz) has narrower tails than traditional recordings, which is another source of its superior performance.

1.2. Chopper stabilization

Chopper stabilization is a common method for the reduction of ($1/f$ type) electrical noise found in electronic devices and amplifiers by rapidly connecting and disconnecting (i.e. chopping) the signal to and from the amplifier input (Enz and Temes, 1996). Chopping (rectangular, 50% duty cycle) shifts a significant portion (25%) of the signal energy to the chop frequency and harmonics where there is less noise. In the case of antennal voltage measurements, low frequency noise arising from the antenna itself, rather than amplifier noise, interferes with the EAG signal. Because insects can respond to odor within milliseconds (French and Meisner, 2007; Schuckel et al., 2008), the EAD output to be moved to a lower noise portion of the frequency spectrum in much the same way. In a preliminary design, we chop the effluent over the antenna by waving two parallel air/effluent mixing tubes in front of antennae at 8 Hz, only one of which draws in the GC effluent. This way, alternating effluent-laden air and clean air are passed over the antenna.

Fig. 2 illustrates chopper stabilization in the time and frequency domains. Panels A, B and C illustrate chopper stabilization in the time domain. The bottom of panel A shows a traditional Gaussian-shaped signal pulse (in this case the GC effluent) corrupted by synthesized Brownian type Gaussian noise. However, the signal may be chopped instead of transduced directly. In a linear sensor, chopping will result in the waveform at the bottom of panel B. The

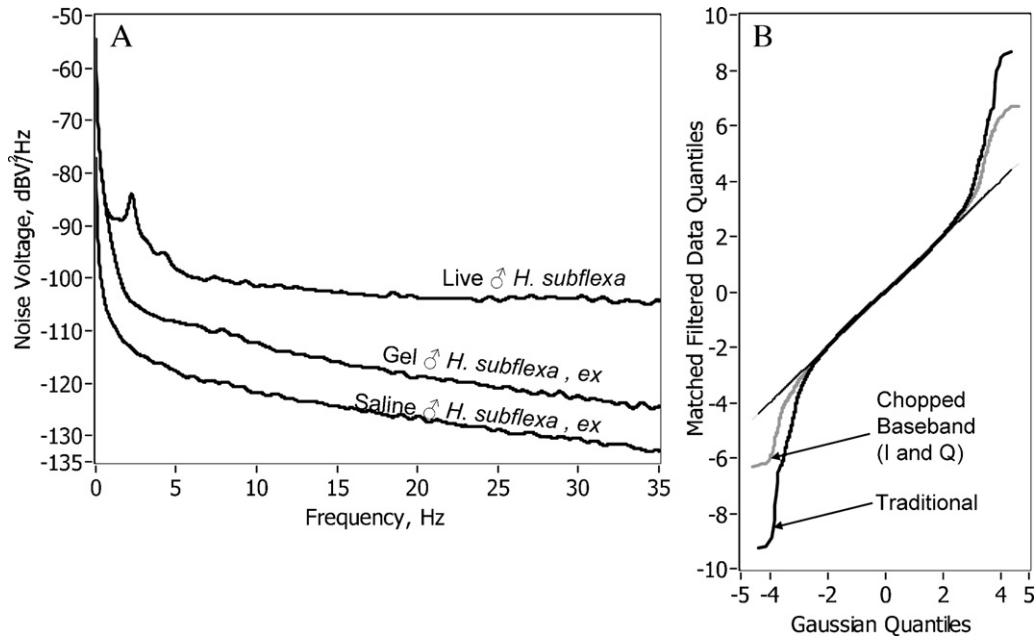


Fig. 1. EAG noise characteristics. (A) Typical noise spectral densities for three types of preparations. ex stands for excised. Spectra are computed using the Yule-Walker method with 100 coefficients on segments 950 s in length acquired at a sample rate of 100 Sa/s. Anti-aliasing filter is at 40 Hz. (B) Q–Q plot illustrating non-Gaussian tails of EAG recordings.

low frequency noise can then be filtered out while retaining only the signal and the low power noise near the chop frequency. Such a waveform is shown at the top of panel C. To recover the baseband signal, the filtered signal is amplitude demodulated, the result of which in the time domain is shown at the bottom of panel C. This signal is higher in quality than the traditional signal shown at the bottom of panel A. Conceptualized energy spectra corresponding to panels A and B are shown in panels D and E. After chopping, the

signal energy in the frequency domain around the chop frequency is seen to be higher in comparison to the noise.

Ideally, chopping simply moves the signal up to the chop frequency (and odd harmonics). In practice, generally, some amount of background chop waveform will be generated even in the absence of signal. Techniques to suppress the chop carrier are desirable and possible. A more stable mechanical implementation is underway for this purpose.

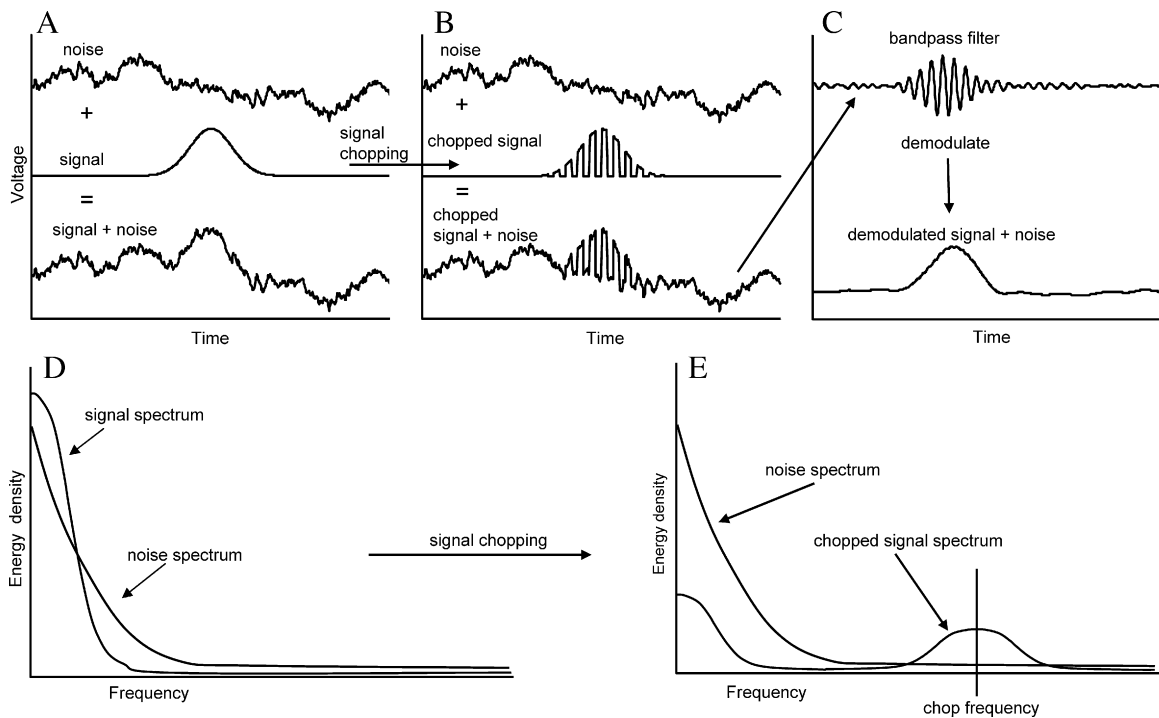


Fig. 2. Chopper stabilization illustrated. (A) Brownian type noise waveform, signal waveform, and their sum. (B) Brownian noise waveform, chopped signal and their sum. (C) Bandpass filtered chopped signal plus noise waveform showing lower noise at the chop frequency and the demodulated signal. (D) Conceptual energy spectral densities for both noise and signal corresponding to panel A. (E) Conceptual energy spectral densities for noise and chopped signal, corresponding to panel B.

2. Theory

2.1. Signal estimation using matched filtering in colored noise

A matched filtering operation has been implemented here for the purpose of EAD amplitude estimation. The maximum likelihood estimate (MLE) of the location (in time) and complex amplitude, a , of a signal mixed with colored Gaussian noise is given by the maximum of a properly scaled matched filter output (Helstrom, 1960, p. 208). In addition, continuous-time matched filtering maximizes SNR for a known signal shape and at a known time in colored Gaussian noise (Moon and Stirling, 2000, p. 215).

The ideal continuous-time matched filter, in theory, may be infinite in length and therefore does not directly apply to a sampled, finite-length recording. If the covariance function of the noise was somehow known exactly, an optimal filter for a finite-length recording may also be constructed (Srinath and Rajasekaran, 1979). However, the exact covariance is not known and must be estimated from the data. Given these circumstances, and that under practical considerations much of the energy of the impulse response of the matched filter may be contained within a suitable time window, it is preferable to approximate the matched filtering operation given a finite number of samples in the recording using a time invariant finite impulse response (FIR) digital filter. Fortunately, the desirable properties of the ideal continuous-time matched filter are also present in the FIR matched filter. For a given length, the FIR matched filter corresponding to a known signal and noise covariance matrix maximizes the SNR (Martinez and Thomas, 1986). Here we use a FIR matched filter as an approximation to the full (but impossible to implement) matched filtering operation.

Conveniently, both the traditional and chopped waveforms may be treated in the same framework. In the signal band (about the fundamental chop frequency, f_c , in the sampled EAG waveform), the observed random process, $x[n]$, is assumed to be the sum of a modulated signal waveform $s[n]$ and a colored narrowband noise process, $v[n]$.

$$x[n] = \text{Re}\{as[n - \tau] + v[n]e^{jnT2\pi f_c}\} \quad (1)$$

where n is an integer enumerating the samples, T is the sample interval, and a is the complex signal amplitude reflecting the antennal gain. $s(t)$ is the normalized envelope of the signal model which is delayed by τ samples and $v[n]$ is the complex envelope of the noise. Note there is only one modulation frequency; here information available from chop frequency harmonics is not utilized. In the case of traditional EAD waveforms, the modulation frequency is 0 and a is real. The conventional method for processing band-pass waveforms is to convert the relevant passband to baseband in complex envelope form. This is achieved via a bandpass filter followed by a complex product detector and a lowpass filter (Trees, 2001). After down-conversion of the signal, the following equation describes the baseband waveform model,

$$x_b[n] = as[n - \tau] + v[n], \quad (2)$$

where the quantities involved are in general, complex. The output of the matched filter may be written in the form

$$x_f[n] = \sum_{m=n}^{n+K-1} h_M[n - m]x_b[m] \quad 0 \leq n < N - K \quad (3)$$

where $h_M[n]$ is the pulse response of the matched filter, K is the length of the filter and N is the length of the recording.

The discrete matched filter sequence can be represented as a vector rather than a time series so that it may be more easily computed. Let \mathbf{x}_b be the vector of length K $[x_b[n] \dots x_b[n + K - 1]]^T$. \mathbf{M} is the true complex covariance matrix of the noise, (which here is estimated from its autocovariance), and \mathbf{s} is the signal vector. The

MLE of the complex amplitude of the signal (when τ is known) is given by a scaled version of the matched filter output (Robey et al., 1992).

$$\hat{a} = \frac{\mathbf{s}^\dagger \mathbf{M}^{-1} \mathbf{x}_b \tau}{\mathbf{s}^\dagger \mathbf{M}^{-1} \mathbf{s}} \quad (4)$$

As in Helstrom (1960), The MLE of the signal magnitude with unknown (discrete) τ may be obtained through a peak search on the filtered data. Thus,

$$|\hat{a}| = \max_n \left| \frac{\mathbf{s}^\dagger \mathbf{M}^{-1} \mathbf{x}_b n}{\mathbf{s}^\dagger \mathbf{M}^{-1} \mathbf{s}} \right| = \left| \frac{1}{\mathbf{s}^\dagger \mathbf{M}^{-1} \mathbf{s}} \right| \max_n \left| (\mathbf{M}^{-1} \mathbf{s})^\dagger \mathbf{x}_b n \right| \quad (5)$$

The coefficients of the FIR filter in (3), $h_M[n]$, then has elements that are contained in the vector $(\mathbf{M}^{-1} \mathbf{s})^\dagger$, which can be obtained by solving the linear system

$$\mathbf{M} \mathbf{q}^* = \mathbf{s} \quad (6)$$

The coefficients of the filter are given by $h_M[n] = \{q_{k-1}, q_{k-2} \dots q_0\}$. For modeling purposes, estimation of the normalized magnitude of the signal, a_N , is used here. a_N is given by the magnitude of a divided by the root mean square (RMS) value of matched-filtered noise alone, δ_{vm} .

$$a_N = \frac{|a|}{\delta_{vm}} \quad (7)$$

The RMS value of the matched filtered noise is estimated from a segment of $x_f[n]$ that does not contain signal from $n = S_1$ to S_2 .

$$\hat{\delta}_{vm} = \sqrt{\frac{1}{S_2 - S_1 + 1} \sum_{n=S_1}^{S_2} |x_f[n]|^2} \quad (8)$$

An estimate of a_N can then be given by the following equation.

$$\hat{a}_N = \frac{\max_n |x_f[n]|}{\sqrt{\frac{1}{S_2 - S_1 + 1} \sum_{n=S_1}^{S_2} |x_f[n]|^2}} \quad (9)$$

Although the numerator in (9) is the MLE, it is generally biased, especially at low SNR.

3. Methods

Dose-response estimates of a_N on both traditional and chopped recordings on live antennal preparations with electroconductive gel connections were made. For both chopped and traditional preparations, three trials at six dosages of Z11-16:Ald were conducted on male antennae of *H. zea*. Dosages are based on an assumed 1:2 split ratio between the FID and the EAD preparation; for each trial, two μL of each dosage were injected into the GC inlet. For chopped preparations, increasing dosages of Z11-16:Ald applied were 0.01 pg, 0.033 pg, 0.1 pg, 0.33 pg, 1.0 pg, and 3.3 pg. On traditional preparations, dosages applied were 33 pg, 100 pg, 330 pg, 1000 pg, 3300 pg and 10000 pg.

3.1. Gas-chromatograph settings

An Agilent 6190N GC was operated in splitless mode using an Agilent HP-5 column, 30 m in length, 0.32 mm dia., with a 0.25 μm internal coating. The GC was operated in constant pressure mode with a flow rate of 2.5 mL/min helium carrier gas at 40 °C (10.9 PSI). The oven temperature was held at 40 °C for 3 min, ramped to 220 °C at 50 °C/min, held at 220 °C from 6.6 to 10.1 min and then ramped to 300 °C for a 4 min bakeout period. The inlet and FID detector were held at 300 °C.

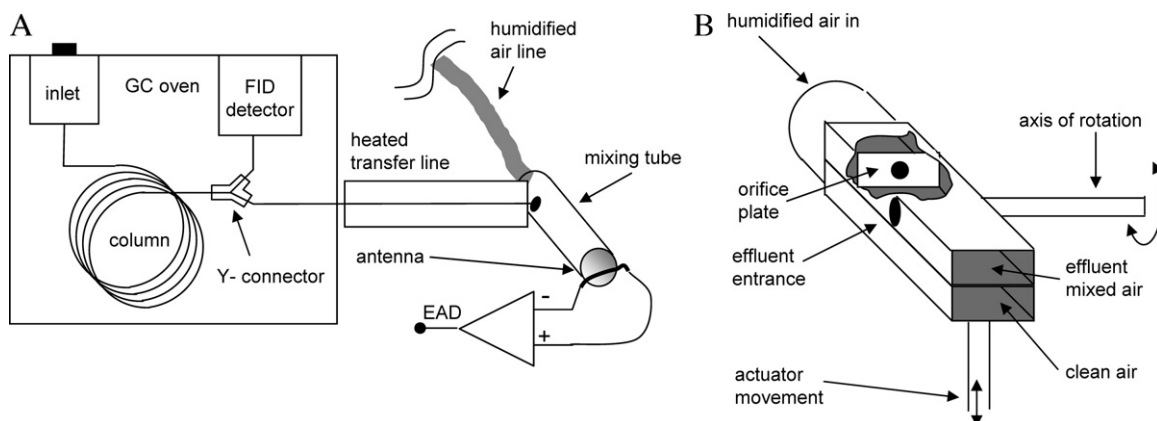


Fig. 3. GC-EAD setup. A. Conventional GC-EAD setup used in this experiment. The GC effluent is split between the FID and antennal preparation. B. Effluent-chopping mixing tube illustration.

3.2. Conventional EAD method

In general, the GC-EAD is generated by routing part of the heated GC effluent into a humidified-air mixing tube and placing the antenna at or near the exiting end of the mixing tube (Schiestl and Marion-Poll, 2002; Struble and Arn, 1984). A cartoon detailing our setup is shown in Fig. 3(A). The column was split 1:1 (FID:EAD) through a fused silica Y connector (Supelco). The transfer line assembly, held at 300 °C, and mixing tube was purchased from Syntech (The Netherlands, Type EC-03-300). “House” air was bubbled at between 1500 mL/min and 3000 mL/min through distilled water and through the Syntech stainless steel mixing tube.

3.3. Effluent chopper implementation

The effluent chopper pictured in Fig. 3(B) was found to be adequate for demonstrating the effectiveness of chopping for EAD recording. The dual flow channel was created using two rectangular brass tubes (3 mm × 7 mm × 150 mm) that were attached to each other using solder. A round brass air-input tube was soldered to the back of these two rectangular tubes. In the side of one of the rectangular tubes, a small 2.38 mm (3/32 in.) dia. effluent entrance hole was drilled. Inside of the rectangular tubes (both tubes to provide symmetry) just before the effluent entrance a 2.38 mm (3/32 in.) dia. orifice plate was placed to generate low pressure at the effluent entrance. This low pressure acted to draw in effluent from the heated transfer line. The device was hinged about a brass axis rod soldered directly across from the effluent entrance hole. At the air exit end on the bottom channel, another brass stub was soldered which was attached via a short piece of removable silicone tubing to the actuator (an audio speaker). The signal to drive speaker actuator was generated using a separate PC running a compiled program written in Labview 8.6 and a DAC output from a National Instruments NI-USB 6212.

3.4. Antennal preparations

Live *H. zea* moths were immobilized in a tapered plastic 1000 μ L pipette tube that had part of the narrow tip removed and ventilation slots cut into it in the axial direction. At the narrow end where the head protruded, an antenna was pulled out of the tube so that it was free to move. The pipette was placed in a holder attached to the preamplifier where a tungsten ground electrode was inserted into the eye on the opposite side of the free antenna. The free antenna was fixed to a gold plated amplifier input electrode using electroconductive gel (Spectra 360 electrode gel, Parker Laboratories,

Fairfield, NJ). The moth was then placed in the mixer effluent so that it was directed over the antenna from front to back.

3.5. EAD recording system

The system described in Myrick et al. (2008) with three of the four channels grounded was used to record signals from live moths and in exploratory measurements. After the data were sampled at 50 kSa/s, a sharp digital anti-aliasing filter with a cutoff frequency of 40 Hz (rather than 25 Hz as in Myrick et al. (2008)) was employed before the data were decimated to 100 Sa/s and written to disk.

3.6. Choice of chop frequency

Several difficulties in characterizing an antennal response are presented by its non-linear and time-variant behavior as a transducer. Because of the complexity in modeling the antenna-chopper system, and our goal of simply demonstrating the chopping technique, we did not address this complexity prior to gathering the results. The chop frequency, 8 Hz, was chosen as a result of an ad-hoc exploratory frequency-swept measurement on several excised gel-connected male *H. zea* antennae. Although approximate, these measurements indicated that small-signal SNR might be maximized in the range of 5 to 8 Hz using major pheromone component, Z11-16:Ald at concentrations well above the detection limit.

3.7. Signal demodulation

The demodulated signals were obtained using direct digital down conversion incorporating two product detectors (Ziemer and Tranter, 1995). The reference clocks of the acquisition system and the DAC were sufficiently close in frequency that no reference signal was necessary to demodulate the recorded signals. An IIR Butterworth 10th order bandpass filter, 4 to 12 Hz, was used to establish a signal band. Product detectors followed by 5th order infinite impulse response (IIR) Butterworth lowpass filters with 3 dB cutoff frequencies of 5 Hz established the baseband in-phase (I) and quadrature (Q) signals. Following this, the baseband signals were decimated to 10 Sa/s. The mean of the noise segment was then subtracted from both I and Q signals and the matched filter was constructed. Although the bandwidth of the signals was 5 Hz, aliased components were negligibly small within the passband of the matched filter.

3.8. Matched filter implementation: noise and signal models

3.8.1. Noise model

To create the matched filter from (6), both a noise model and a signal model are necessary. The noise autocovariance was computed using the “biased” method (Proakis et al., 2002).

$$\hat{\gamma}_{vv}[k] = \frac{1}{N} \sum_{n=0}^{N-k-1} v[n]v^*[n+k], \quad (10)$$

where $\hat{\gamma}_{vv}[k]$ is the autocovariance sequence. Assuming the noise is stationary and ergodic, the autocovariance was used to estimate the entire covariance matrix, \mathbf{M} .

3.8.2. Signal models

The signal models differed depending on the recording type. Although FID peaks for large amounts of Z11-16:Ald were consistently Gaussian in shape, the transduced signal at the antenna is modified by effects such as peak tailing and the low frequency transfer function of the antenna. The term transfer function is used loosely because the response of the antenna is non-linear. Signal models described below were created in 40 s windows, from a Gaussian shaped pulse centered at 20 s.

3.8.2.1. Chopped recordings signal model. The signal model for chopped recordings was a Gaussian shaped pulse passed through a single pole lowpass filter used to model peak tailing. The transfer function of the lowpass filter is given by the following equation

$$H(z) = \frac{1}{1 - \exp(-1/\tau_p f_s)z^{-1}} \quad (11)$$

where f_s is the sampling frequency in Sa/s and τ_p is the “peak-tailing” time constant in seconds. See Fig. 4(A) for a representative model and recording.

3.8.2.2. Traditional GC-EAD signal model. The signal model for traditional recordings is a Gaussian-shaped pulse passed through both the single pole peak-tailing lowpass filter given by (11) and then a highpass filter digitally equivalent (step invariant) to the highpass filter used in the acquisition system. Its transfer function is given by the following equation.

$$H(z) = \frac{1 - z^{-1}}{1 - \exp(-1/\tau_f f_s)z^{-1}} \quad (12)$$

where τ_f is the time constant, in seconds, associated with the high-pass filter. An example recording and the signal model are shown in Fig. 4(B).

The better the fit of the waveform to the signal, the higher the SNR (on average) that will be obtained when it is calculated. The full width half maximum (FWHM) value assigned to the Gaussian pulse consistently increased the SNR obtained in both chopped and traditional recordings. The peak tailing time constant was chosen as a result of the observation of several chopped recordings. The same peak tailing constant obtained from the chopped recordings was used in the traditional signal models.

Parameters used for signal and noise modeling used the noise segment from 200 to 500 s to calculate the autocovariance, the Gaussian pulse input was modeled with a FWHM value of 4 s, the peak tailing time constant was 10 s and the highpass time constant of 1.06 s was used, corresponding to that of the acquisition system.

3.9. Measurements

A peak search was performed within a 5 s window where the peak was expected to elute. Each traditional normalized amplitude estimate has an uncertainty due to noise, excluding modeling errors and uncertainties, of approximately ± 1 V/V (i.e. 1 standard deviation). Some bias in the estimate, up to about +0.3 V/V, is also present at low SNR. Uncertainty in chopped normalized estimates is about ± 0.707 V/V due to noise.

4. Results

Recordings obtained from trial 3 (see Table 1) of both the chopped and traditional experiments are displayed in Fig. 5. It is clearly evident that the quality of the recordings obtained from chopping is superior to those obtained using traditional methods. The raw demodulated chopped recordings of Fig. 5(C) are undistorted by the highpass filtering necessary to remove baseline drift in raw traditional recordings of Fig. 5(A).

Evident on the chopped recordings is peak tailing that is not readily visible in the traditional recordings. It is likely the peak tailing is due to condensation inside the GC column as it exits the transfer line. In experiments conducted under more ideal conditions for making traditional measurements, (Myrick and Baker, in preparation) peak tailing was reduced by shortening the length of column at the exit of the transfer line.

Matched filtering applied to the recordings results in the waveforms shown in Fig. 5(B) and (D). It should be noted that matched filtering is only designed with one signal and one stationary noise model, thus it is unable to screen out sharp non-Gaussian deviations from the baseline from signal. The matched filter is scaled to estimate the amplitude of the Gaussian-shaped input waveform,

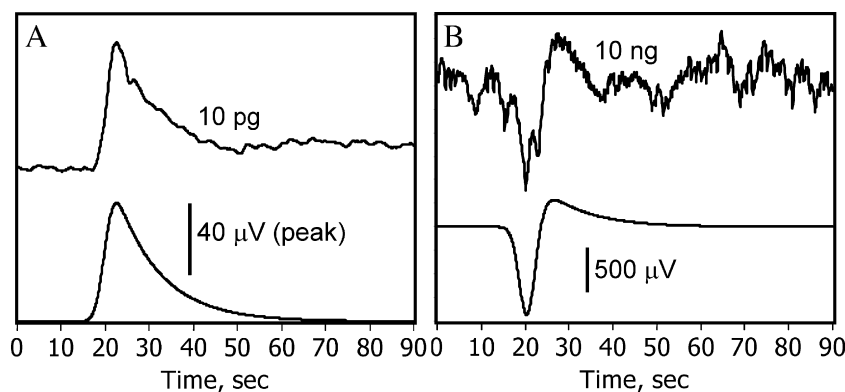


Fig. 4. Signal models. (A) Upper trace: estimated in-phase signal component of a demodulated chopped recording decimated to 10 Sa/s. Lower trace: chopped signal model with amplitude estimated from (5) applied to the upper trace. (B) Upper trace: traditional recording decimated to 10 Sa/s. Dosage is indicated. Lower trace: traditional signal model with amplitude estimated from (5) applied to the upper trace.

Table 1
Dose–response estimates of normalized amplitude \hat{a}_N .

Dosage (pg)	Traditional \hat{a}_N				Dosage (pg)	Chopped \hat{a}_N			
	Trial 1	Trial 2	Trial 3	Mean \pm SE		Trial 1	Trial 2	Trial 3	Mean \pm SE
33	2.50	1.57	1.12	1.73 \pm 0.41	0.010	1.13	1.16	1.40	1.23 \pm 0.07
100	1.66	3.39	4.08	3.04 \pm 0.72	0.033	1.55	2.23	8.31	4.03 \pm 1.75
330	2.30	3.18	4.92	3.47 \pm 0.77	0.10	5.18	10.5	8.22	7.96 \pm 1.26
1000	5.56	6.24	6.24	6.01 \pm 0.23	0.33	9.79	8.85	27.5	15.4 \pm 4.9
3300	4.56	5.30	7.68	5.85 \pm 0.94	1.0	11.7	6.26	31.0	16.3 \pm 6.1
10000	5.59	4.88	6.30	5.59 \pm 0.41	3.3	18.0	14.2	37.3	23.2 \pm 5.8

whose size is greatly reduced by the peak tailing constant and high-pass filters used in the signal model. As a result, the estimate of the size of the Gaussian input is much larger than the peaks seen in the raw recordings. A clear advantage of using matched filtering on traditional waveforms is not evident, mainly because the signal occupies a very high noise portion of the EAD noise spectrum. Matched filtering applied to the chopped recordings is successful in removing low frequency drift and higher frequency noise components.

Estimates of a_N made for each waveform are summarized in Table 1, where an approximate estimate of the performance

increase can be inferred. The traditional dosage of 100 pg has expected normalized amplitude in the range from 2.3 to 3.8, corresponding to the lower range of a_N found at the chopped dosage of 0.033 pg ($<10^4$ ratio in dosage). The traditional dosage of 330 pg (2.7 to 4.2) has similar normalized amplitude as the chopped dosage of 0.033 pg (10^4 ratio in dosage). A traditional dosage of 1000 pg (5.8 to 6.2) translates to somewhere between 0.033 and 0.10 pg (6.7 to 9.2) chopped ($>10^4$ ratio in dosage). We also analyzed these data using methods outlined in Myrick and Baker (in preparation) to estimate the limit of detection associated with a 5% naïve error

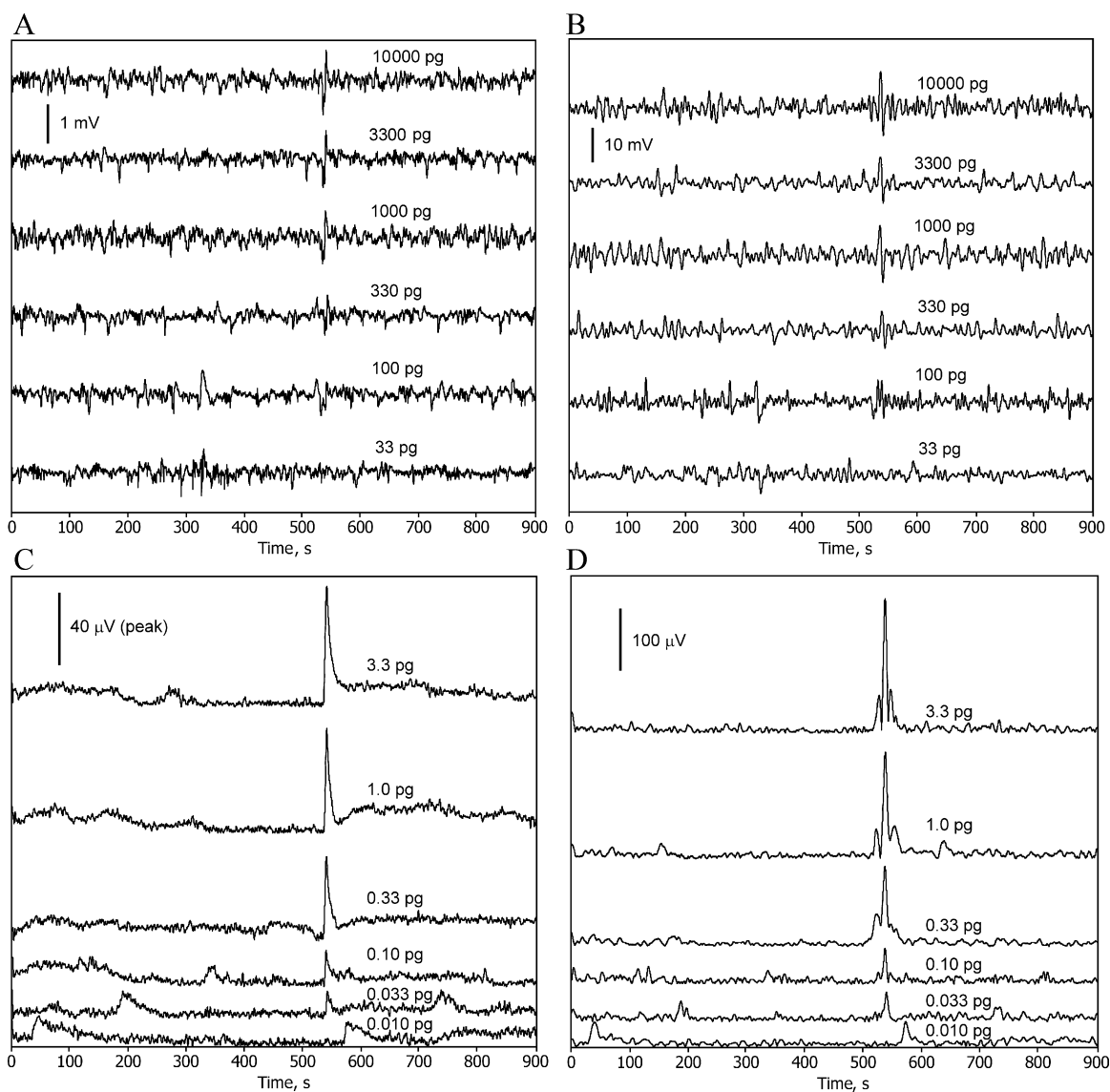


Fig. 5. Traditional and chopped live *H. zea* pheromone dose–response EAD recordings. Z11-16:Ald odorant elutes at 540 s. Vertical scale and dosages are labeled. (A) traditional, (B) traditional matched, (C) chopped and demodulated without matched filtering, (D) chopped and demodulated with matched filtering.

rate. Given the measurements and a uniform prior probability density of the logarithm of the dosage, the inferred probability density of the detection limit ranges from 832 to 4365 pg from the 15th to 85th percentile, having a median value of 1479 pg and a most likely value of around 1100 pg. When the dosage has a uniform prior density on a linear scale, making higher dosages more likely, the method is unable to make similar estimates due to the low number of measurements. However the most likely value in that case can be estimated and is around 1800 pg. The chopped method is predicted to have a detection limit in the 15th to 85th percentile range from 0.144 to 0.776 pg with a median value of 0.257 pg and a most likely value around 0.19 pg. With a uniform linear dosage prior density, the most likely value is around 0.30 pg. Thus we conclude in this case that a performance increase of around 10^4 was achieved. The large performance increase is contributed to by the large amount of noise in live recordings in conjunction with the long time course of the GC-EAD peak. Another result of interest is the smaller standard error in traditional recordings compared to chopped recordings. This could be because at the high dosages, the antennae are more fully saturated and differences between individuals become more evident at the lower dosages.

5. Conclusions

We have introduced a technique to increase SNR in EAD recordings by chopping the GC effluent passing over the antenna and applied matched filtering to the resulting waveforms to maximize SNR. Chopper stabilization at 8 Hz is estimated to increase the sensitivity of the instrument by approximately a factor of 10^4 in live whole animal *H. zea* antennal preparations made with electroconductive gel connections to the amplifier. The dramatic increase in performance possibly makes the method well suited to measurements on very small insects where live preparations must be used and signals may be noisy. However, the maximum improvement in SNR is not being achieved by the current chopper configuration. Noise is also added by the chopper around the carrier frequency where the signal will appear. We believe the noise is produced by variability in the chopping action over time coupled with a strong background carrier signal, in addition to antennal aging. The background signal could be the result of mechanical disturbances and/or different temperature distributions passing over the antenna. If the mechanical disturbances can be removed, the carrier noise can be reduced, further increasing the SNR that is currently being achieved. Information is also available at harmonics of the chop frequency. It may be possible to include analysis of harmonics in future methods. Investigation into the effect of modulation frequency content on different preparation types and antennal species with different compounds and concentrations would likely become useful for improvement in making GC-EAD measurements.

Acknowledgements

The authors gratefully acknowledge funding from the Office of Naval Research (Counter-IED Program), and the Defense Threat

Reduction Agency (New Concepts in Nano-scale Chemical and Biological Sensing) that supported this research. The ONR and DTRA played no role in the design of the experiments; nor did they play any role in data collection, data analysis, interpretation of results, the writing of the report, or the decision to publish these findings.

References

- Dolzer, J., Fischer, K., Stengl, M., 2003. *J. Exp. Biol.* 206, 1575–1588.
- Enz, C.C., Temes, G.C., 1996. *P. IEEE* 84 (11).
- French, A.S., Meisner, S., 2007. *Chem. Senses* 32, 681–688.
- Gouinguen e, S., Cruz, I.d., Pers, J.v.d., Wadhams, L., Marion-Poll, F., 1998. *Chem. Senses* 23, 647–652.
- Gu edot, C., Landolt, P.J., Smithhisler, C.L., 2008. *Fla. Entomol.* 91, 576–582.
- Helstrom, C.W., 1960. *Statistical Theory of Signal Detection*. Pergamon Press, New York.
- Kaissling, K.-E., 1995. In: Spielman, A.I., Brand, J.G. (Eds.), *Experimental Cell Biology of Taste and Olfaction*. CRC Press, Boca Raton, FL.
- Kapitskii, S.V., Gribakin, F.G., 1992. *J. Comp. Physiol. A* 170, 651–663.
- Malo, E.A., Renou, M., Guerrero, A., 2000. *Talanta* 52, 525–532.
- Mankin, R.W., Mayer, M.S., 1983. *J. Theor. Biol.* 100, 613–630.
- Martinez, A.B., Thomas, J.B., 1986. *J. Frankl. Inst.* 324 (1), 139–147.
- Moon, T.K., Stirling, W.C., 2000. *Mathematical Methods and Algorithms for Signal Processing*. Prentice-Hall, Upper Saddle River, New Jersey.
- Moorhouse, J.E., Yeadon, R., Beavor, P.S., Nesbitt, B.F., 1969. *Nature* 223, 1174–1175.
- Myrick, A.J., Baker, T.C., in preparation.
- Myrick, A.J., Park, K.-C., Hetling, J.R., Baker, T.C., 2008. *Bioinspir. Biomim.* 3 (4), 046006.
- Olsson, P.-O.C., Anderbrant, O., L ofstedt, C., Borg-Karlson, A.-K., Liblikas, I., 2005. *J. Chem. Ecol.* 31 (12), 2947–2961.
- Park, K.C., Baker, T.C., 2002. *J. Insect Physiol.* 48, 1139–1145.
- Party, V., Hanot, C., Said, I., Rochat, D., Renou, M., 2009. *Chem. Senses* 34, 763–774.
- Patte, F., Etcheto, M., Marfaing, P., Laffort, P., 1989. *J. Insect. Physiol.* 35 (9), 667–675.
- Proakis, J.G., Rader, C.M., Ling, F., Nikias, C.L., Moonen, M., Proudler, I.K., 2002. *Algorithms for Statistical Signal Processing*. Prentice Hall, Upper Saddle River.
- Robey, F.C., Fuhrmann, D.R., Kelly, E.J., Nitzberg, R., 1992. *IEEE Trans. Aero. Electr. Syst.* 28 (1), 208–216.
- Roelofs, W.L., 1984. In: Hummel, H.E., Miller, T.A. (Eds.), *Techniques in Pheromone Research*. Springer-Verlag, New York, pp. 131–159.
- Rospars, J.-P., Krivan, V., Lansky, P., 2000. *Chem. Senses* 25, 293–311.
- Schiestl, F.P., Marion-Poll, F., 2002. In: Jackson, J.F., Linskins, H.F. (Eds.), *Molecular Methods of Plant Analysis. Analysis of Taste and Aroma*, vol. 21. Springer.
- Schneider, D., 1957. *Z. Vergleich. Physiol.* 40, 8–41.
- Schroth, P., L uth, H., Hummel, H.E., Sch utz, S., Sch oning, M.J., 2001a. *Electrochim. Acta* 47, 293–297.
- Schroth, P., Sch oning, M.J., Kordo s, P., Sch utz, S., Wei becker, B., Hummel, H.E., 1999. *Biosens. Bioelectron.*, 303–308.
- Schroth, P., Sch oning, M.J., L uth, H., Wei becker, B., Hummel, H.E., Sch utz, S., 2001b. *Sens. Actuators B* 78, 1–5.
- Schuckel, J., French, A.S., 2008. *J. Neurosci. Methods* 171, 98–103.
- Schuckel, J., Meisner, S., Torkkeli, P.H., French, A.S., 2008. *J. Comp. Physiol. A* 194, 483–489.
- Siderhurst, M.S., Jang, E.B., 2006. *J. Chem. Ecol.* 32, 2513–2524.
- Sillam-Duss es, D., Kalinov a, B., Jiros, P., Brezinov a, A., Cvacka, J., Hanus, R., Sobotnik, J., Bordereau, C., Valterov a, I., 2009. *J. Insect Physiol.* 55 (8), 751–757.
- Sloane, D.H., Sullivan, B.T., 2007. *J. Chem. Ecol.* 33, 1748–1762.
- Srinath, M.D., Rajasekaran, P.K., 1979. *An Introduction to Statistical Signal Processing with Applications*. John Wiley & Sons, New York.
- Stelinski, L.L., Miller, J.R., Gut, L.J., 2003. *J. Chem. Ecol.* 29 (2), 405–423.
- Struble, D.L., Arn, H., 1984. In: Hummel, H.E., Miller, T.A. (Eds.), *Techniques in Pheromone Research*. Springer-Verlag, New York, pp. 161–178.
- Trees, H.L.V., 2001. *Detection, Estimation, and Modulation Theory. Part I. Detection, Estimation and Linear Modulation Theory*. John Wiley & Sons, Inc., New York.
- Zhang, Q.-H., Erbilgin, N., Seybold, S., 2008. *Chemoecology* 18 (4), 243–254.
- Ziegler, C., G opel, W., Hammerle, H., Hatt, H., Jung, G., Laxhuber, L., Schmidt, H.L., Sch utz, S., V ogtle, F., Zell, A., 1998. *Biosens. Bioelectron.* 13, 539–571.
- Ziemer, R.E., Tranter, W.H., 1995. *Principles of Communications Systems, Modulation, and Noise*, Fourth ed. John Wiley & Sons, Inc., New York.